Supplementary material for

The Excellent Performance in Hydrogenation of Esters over Cu/ZrO_2 Catalyst Prepared by Bio-Derived Salicylic Acid

Jian Ding[ab], Yanting Liu[ab], Juan Zhang[a], Kefeng Liu[c], Haicheng Xiao[c], Fanhua Kong[c], Yanping Sun[d], and Jiangang Chen*[a]

[a] State Key Laboratory of Coal Conversion, Shanxi Institute of Coal Chemistry, Chinese Academy of Sciences, Taiyuan 030001, Shanxi, PR China

[b] University of Chinese Academy of Sciences, Beijing 100049, PR China

[c] Petrochemical Research Institute of PetroChina Company Limited, Beijing 100029, PR China

[d] Chemical Engineering Department, Taiyuan University of Technology, Taiyuan 030001, PR China

* Corresponding author. Tel.: +86 0351 4040290; fax: +86 0351 4040290.

E-mail: chenjg@sxicc.ac.cn.

Preparation of the Cu/ZrO_2 catalyst with the aid of bio-derived organic carboxylic acids or not

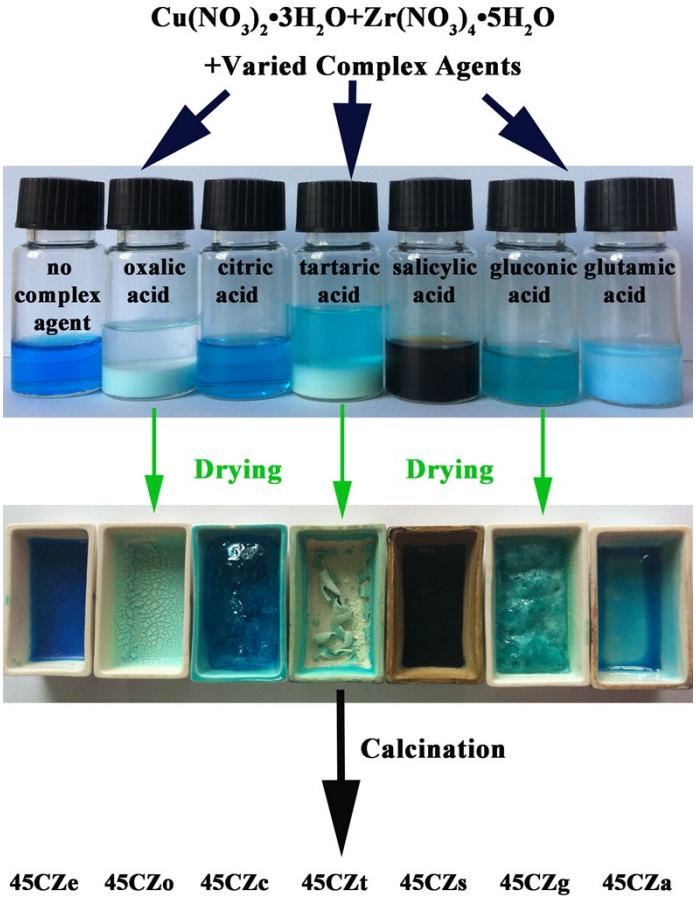

Scheme S1. Schematic view of preparing binary Cu/ZrO_2 catalyst using varied organic carboxylic acids.

The conversion and selectivity of products for the DEO conversion were calculated based on the following equations [Eq. (1-3)]:

$$\text{Conversion} = (1 - \frac{\text{Amount of DEO after reaction (mol)}}{\text{Total amount of DEO in feed (mol)}}) \times 100\% \quad (1)$$

$$\text{Selectivity} = \frac{\text{Amount of a product (mol)}}{\text{Total amount of DEO converted (mol)}} \times 100\% \quad (2)$$

$$STY_{EG} = \frac{Conv.\ of\ DEO \times LHSV \times \rho_{DEO} \times Sel.\ of\ EG \times Molecular\ weight\ of\ EG}{Molecular\ weight\ of\ DEO} (g_{EG}\ g_{cat}^{-1}\ h^{-1})$$

1 (3)

2 The turnover frequency (TOFs), as defined as the number of converted DEO

3 molecules in 1 h over one active site, was calculated based on the following equation:

4
$$TOF^0 = \frac{DEO\ conversion\ rate\ (mol\ g_{cat}^{-1}\ h^{-1})}{Numbers\ of\ Cu\ sites\ (mol\ g_{cat}^{-1})} = \frac{Conv.\ of\ DEO \times LHSV \times \rho_{DEO}\ (g_{DEO}\ g_{cat}^{-1}\ h^{-1})}{Molecular\ weight\ of\ DEO \times Numbers\ of\ Cu\ sites\ (mol\ g_{cat}^{-1})} \quad (4)$$

5 The numbers of surface Cu sites were determined by N_2O nitration. To obtain the

6 intrinsic activity of catalysts, the DEO conversion was kept below 50% and EG yield

7 was kept less than 10% at high WLHSV of 12.0 h^{-1}.

8 **Particle sizes calculated by the Scherer equation**

9 The crystallite sizes were calculated from the line-broadening of the XRD peaks

10 by the Scherrer equation using the (111) peak position [Eq. (5)].

11
$$\boldsymbol{d = \frac{K\lambda}{FW\cos\theta}} \quad (5)$$

12 Where K is a constant generally taken as unity (0.89); λ is the wavelength of the

13 incident radiation (0.15405 nm); FW is the full width at half maximum and θ is the

14 peak position.

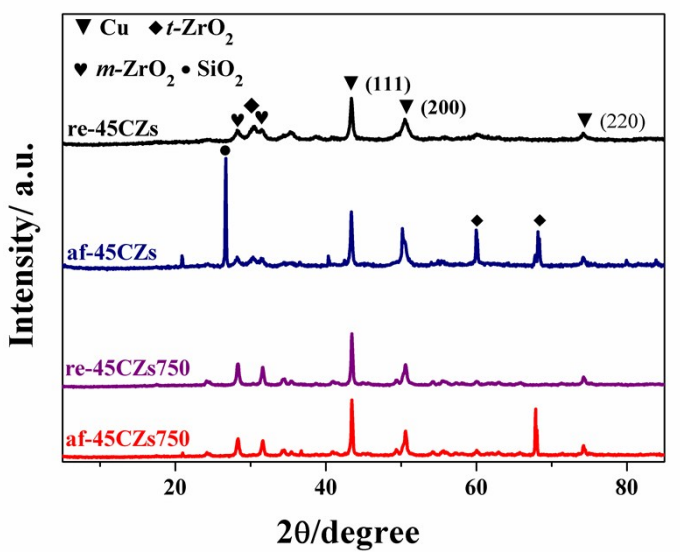

Figure S1. XRD patterns of the pre-reduced catalysts (denoted as re-45CZs and re-45CZs750) and used catalysts after esters hydrogenation (denoted as af-45CZs and af-45CZs750).

The measurement of specific Cu^0 surface areas of the catalysts

The specific surface area of metallic copper was measured by N_2O oxidation and followed H_2 reduction using the procedure described by Van Der Grift et al..[1-3] The procedures described here were performed on a homemade apparatus and the profiles was shown in Figure S2-3.[4] Generally, catalysts (60 mg) were first reduced in 5% H_2/N_2 mixture at a flow rate of 50 mL min^{-1} with a ramping rate of 10 °C min^{-1} until 350 °C. The amount of hydrogen consumption in the first TPR (TPR1) was denoted as X. And then the reactor was purged with Ar to 50 °C. N_2O (30 mL min^{-1}) was injected to oxidize surface copper atoms to Cu_2O at 50 °C for 15 min. Subsequently, the reactor was flushed with Ar to remove the oxidant. Finally, another TPR experiment was performed in 5% H_2/N_2 at a flow rate of 50 mL min^{-1}. Hydrogen consumption in the second TPR (TPR1) was denoted as Y. The dispersion of Cu and exposed Cu surface area were calculated according to the equations which were shown below:

Reduction of all copper atoms:

$CuO + H_2 \rightarrow Cu + H_2O$, hydrogen consumption in the first TPR1 = X.

the decomposition of N_2O on the surface of metallic copper:

$2Cu + N_2O = N_2 + (Cu–O–Cu)s$.

Reduction of surface copper atoms only:

$Cu_2O + H_2 \rightarrow 2Cu + H_2O$, hydrogen consumption in this TPR2 = Y;

And the dispersion of Cu and exposed Cu surface area were calculated as [Eq. (6, 7)]:

$$D = \frac{2Y}{X} \times 100\% \quad (6)$$

$$S = \frac{2Y \times N_{av}}{X \times M_{Cu} \times 1.4 \times 10^{19}} = \frac{1353Y}{X}(m^2 - Cu / g - Cu) \quad (7)$$

where N_{av} is the Avogadro's constant, M_{Cu} is the relative atomic mass (63.5 g mol^{-1}), 1.4×10^{19} comes from that an equal abundance of an average copper surface atom area of 0.0711 nm^2, equivalent to 1.4×10^{19} copper atoms m^{-2}.[3]

Average volume-surface diameter (d_{Cu}) can be expressed as a function [Eq. (8)]:

$$d_{v.s.} = \frac{6}{(S \times \rho_{Cu})} \approx 0.5\frac{X}{Y}(nm) \quad (8)$$

where, ρ_{Cu} is the density of copper (8.9 g cm^{-3}).

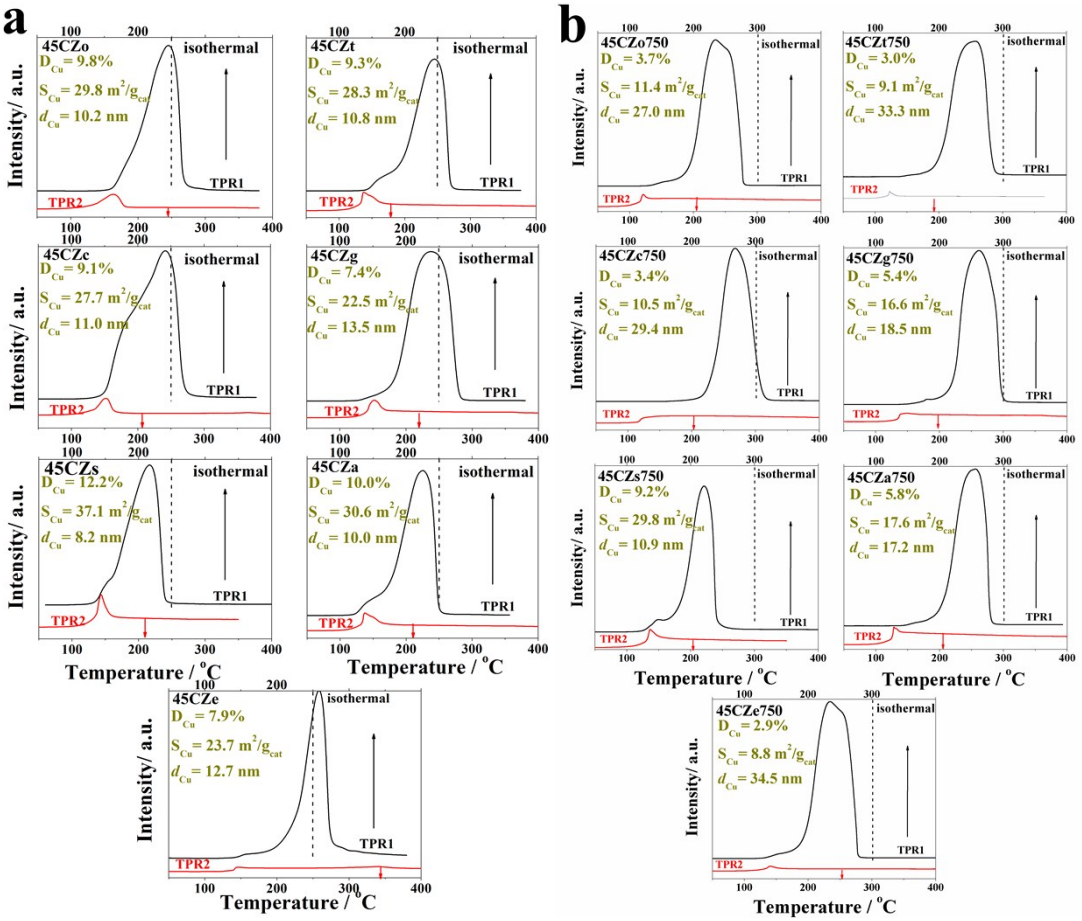

Figure S2. The profiles of Cu metal surface area of (a) 45CZ*x* and (b) 45CZ*x*750 catalysts determined by the N_2O titration method.

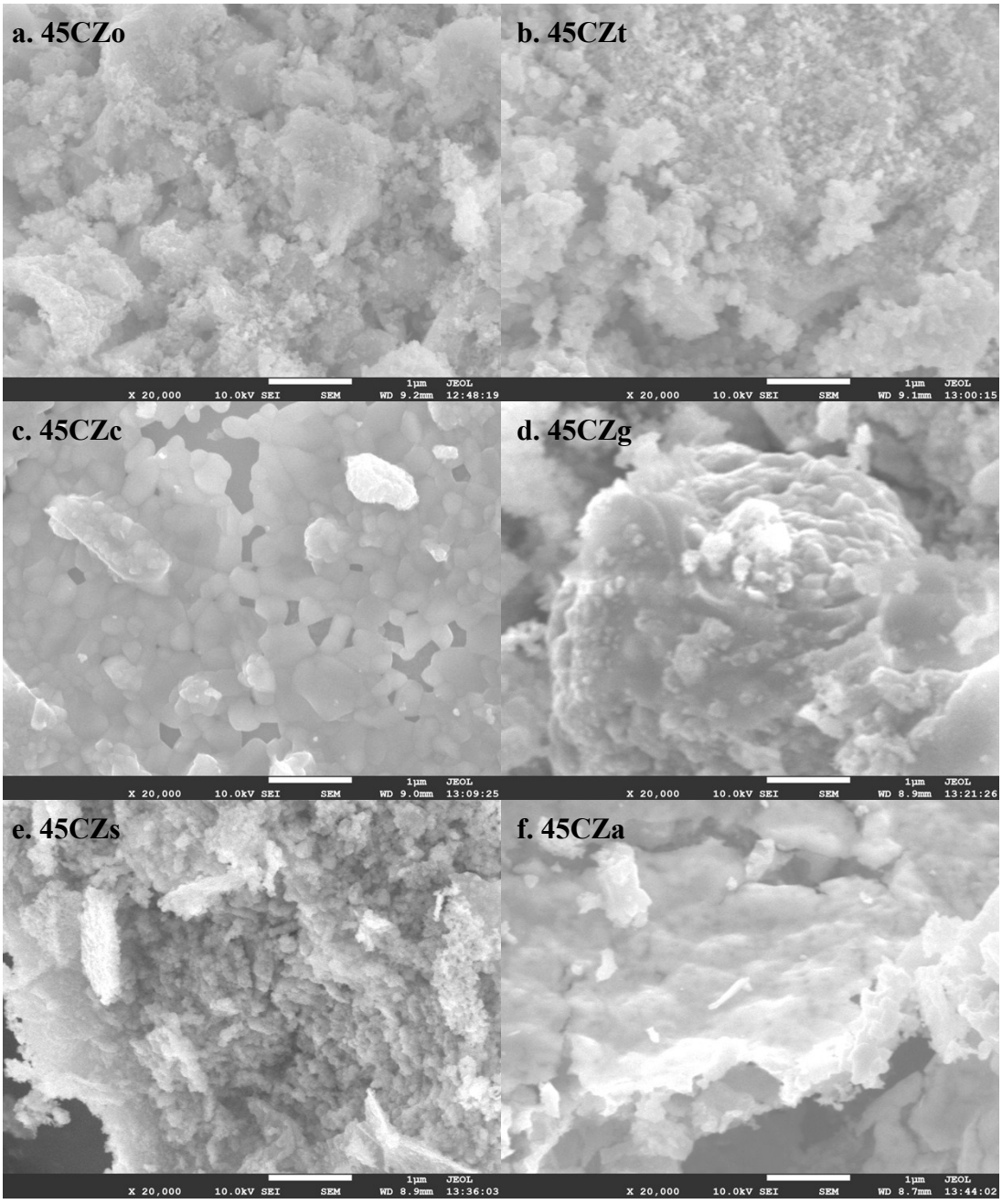

Figure S3. SEM images of the 45CZx catalysts.

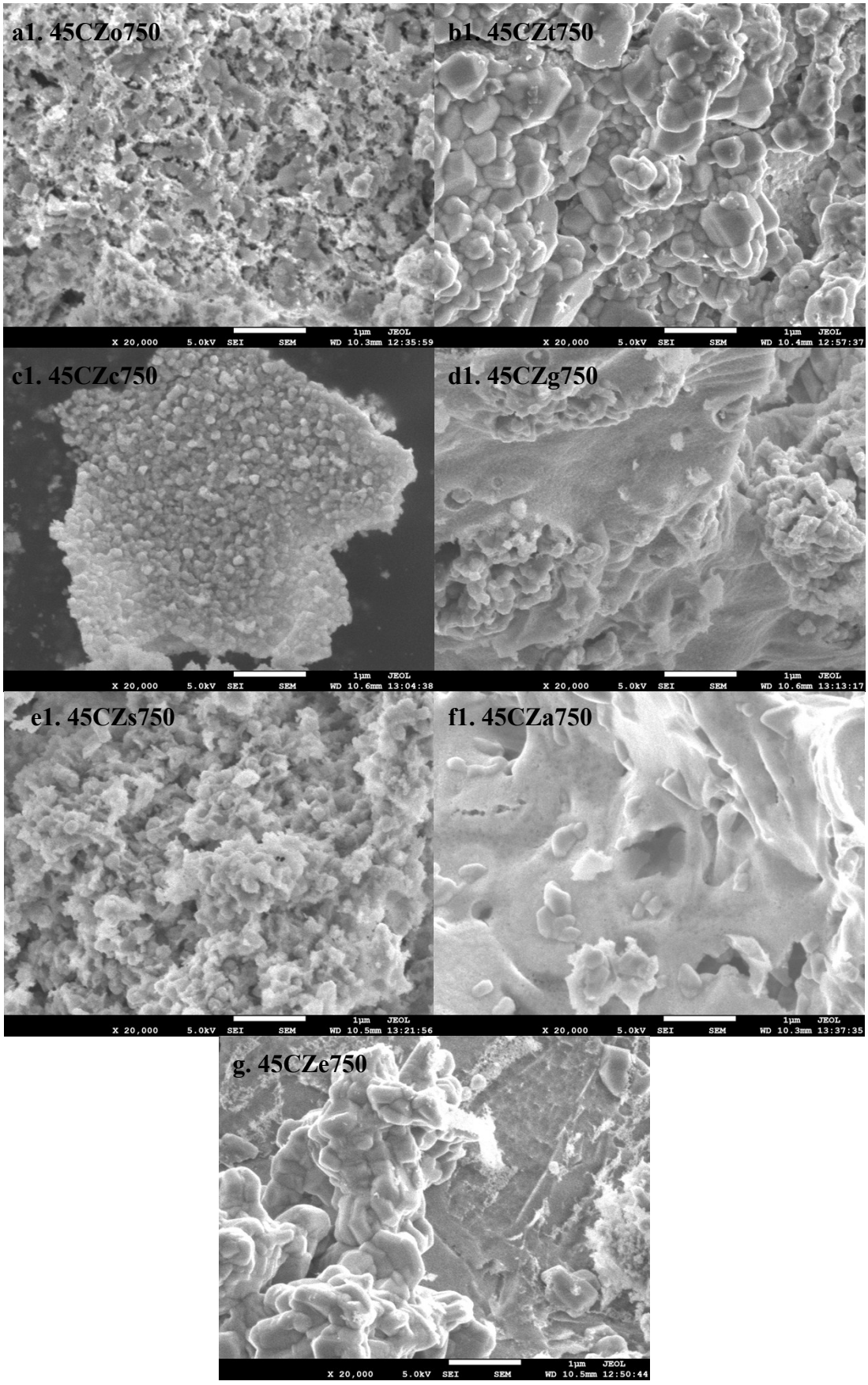

Figure S4. SEM images of the 45CZ*x*750 catalysts.

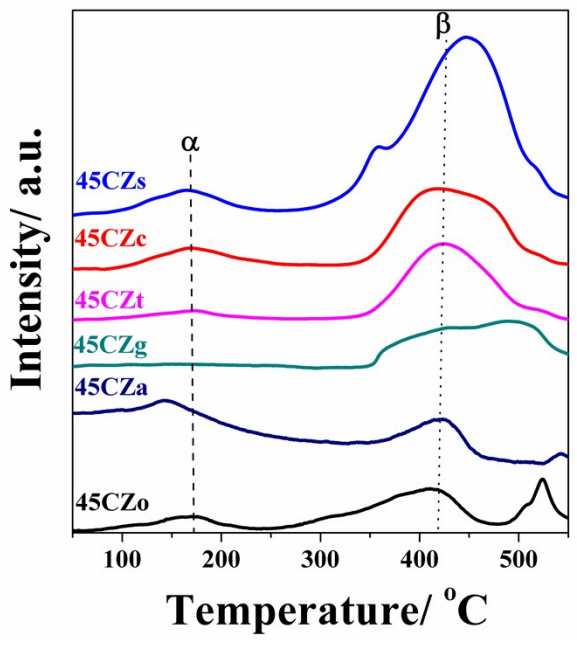

Figure S5. H_2-TPD profiles of the 45CZ*x* catalysts.

The hydrogen activation over the reduced 45CZ*x* catalysts was tested by H_2-TPD and the profiles were shown in Figure S5. Several H_2 desorption peaks appeared for all the samples, which were similar at temperature, but varying greatly in the strength. According to the reports,[5, 6] the resolved peak at low temperature (110–220 °C) could be ascribable to the associative adsorbed H_2 on the highly dispersed Cu.[7, 8] While a much broader signal in the range of 350–500 °C monitored the desorption of hydrogen from the split H–H on the surface of Cu–ZrO_2 interfaces or CuH_x.[9, 10] Interestingly, the intensities of the H_2 desorption peaks of the 45CZ*x* catalysts were closely affected by the complex agent used. Apparently, the peak α enhanced in 45CZs and lowered in other samples, especially absent in 45CZg (curves in Figure S5). It indicated that there were more active sites for associative adsorption of H_2 because of the existing of highly dispersed CuO particles over 45CZs. Frankly, no desorption peak was observed in the low temperature range over 45CZg, which due to lacking the highly

dispersed Cu species as confirmed by XRD and TPR (Figures 1 and 5). Similarly, the H_2 desorption peak β was maximum for 45CZs and was much greater than that of 45CZo, 45CZc, 45CZt, and 45CZa. The huge high-temperature peak β of 45CZs was attributed to the synergism between *t*-ZrO_2 and the Cu active sites for facile H_2 dissociation which was helpful to form CuH_x. Taken together, the H_2 activation ability of 45CZ*x* deduced from TPD profiles followed the sequence of 45CZs> 45CZc> 45CZt> 45CZa> 45CZg> 45CZo. Generally, the catalyst which possessed a higher D_{Cu} and S_{Cu} showed the stronger H_2 desorption peaks both located at ca. 160 and 450 ^oC, implying that surface Cu atoms were highly correlated with the formation of the chemisorbed H species. Moreover, the increasing content of crystalline ZrO_2 can indirectly improve the rate of efficient hydrogen activation and promote the surface concentration of active hydrogen species via the synergism between the Cu species and ZrO_2. It was postulated that these enhanced H_2 activation ability would improve its activity for esters hydrogenation.

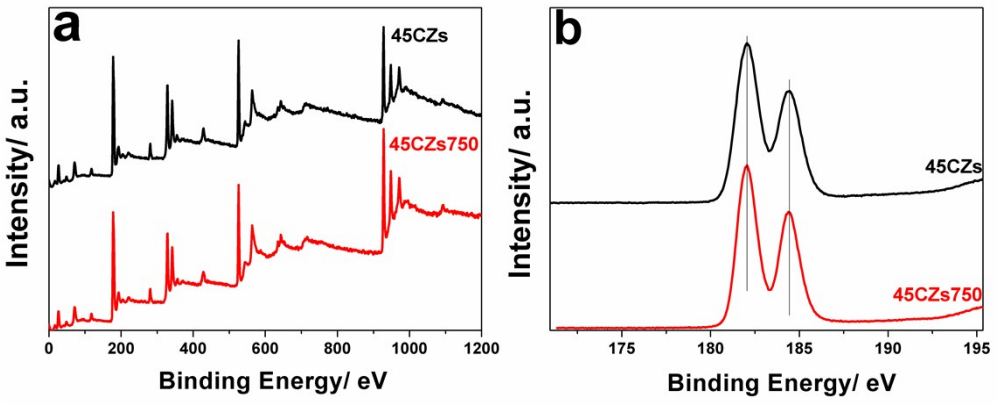

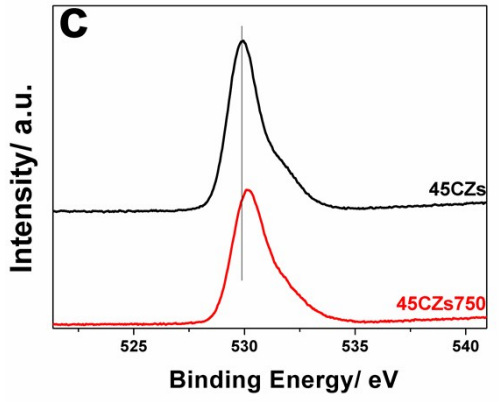

Figure S6. XPS spectra (a), Zr 3d spectra (b), and O 1s spectra (c) of the 45CZs and 45CZs750 catalysts.

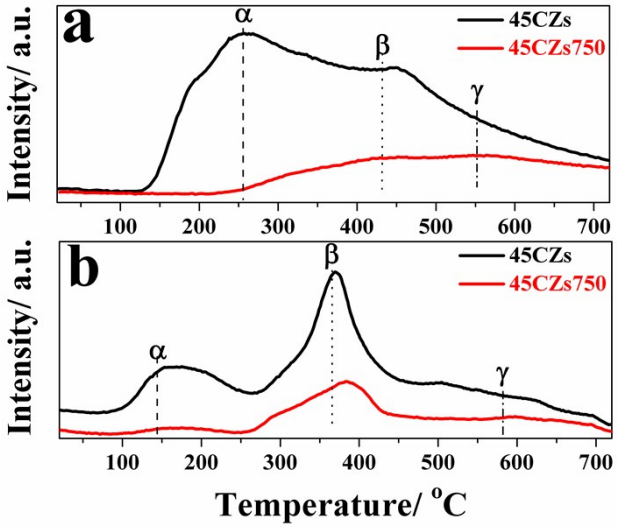

Figure S7. NH_3-TPD (a) and CO_2-TPD (b) profiles of the 45CZs and 45CZs750 catalysts.

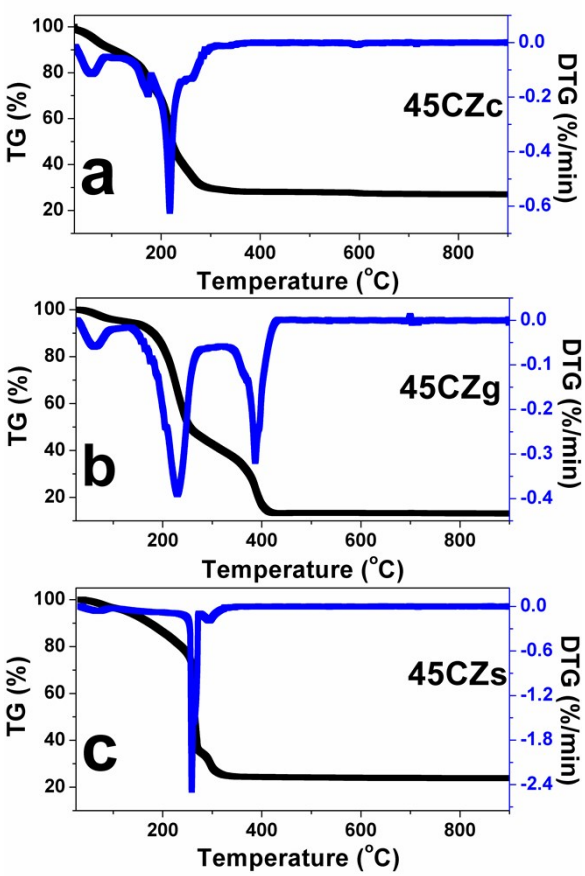

Figure S8. TG and DTG curves for the precursors of (a) 45CZc, (b) 45CZg, and (c) 45CZs catalysts.

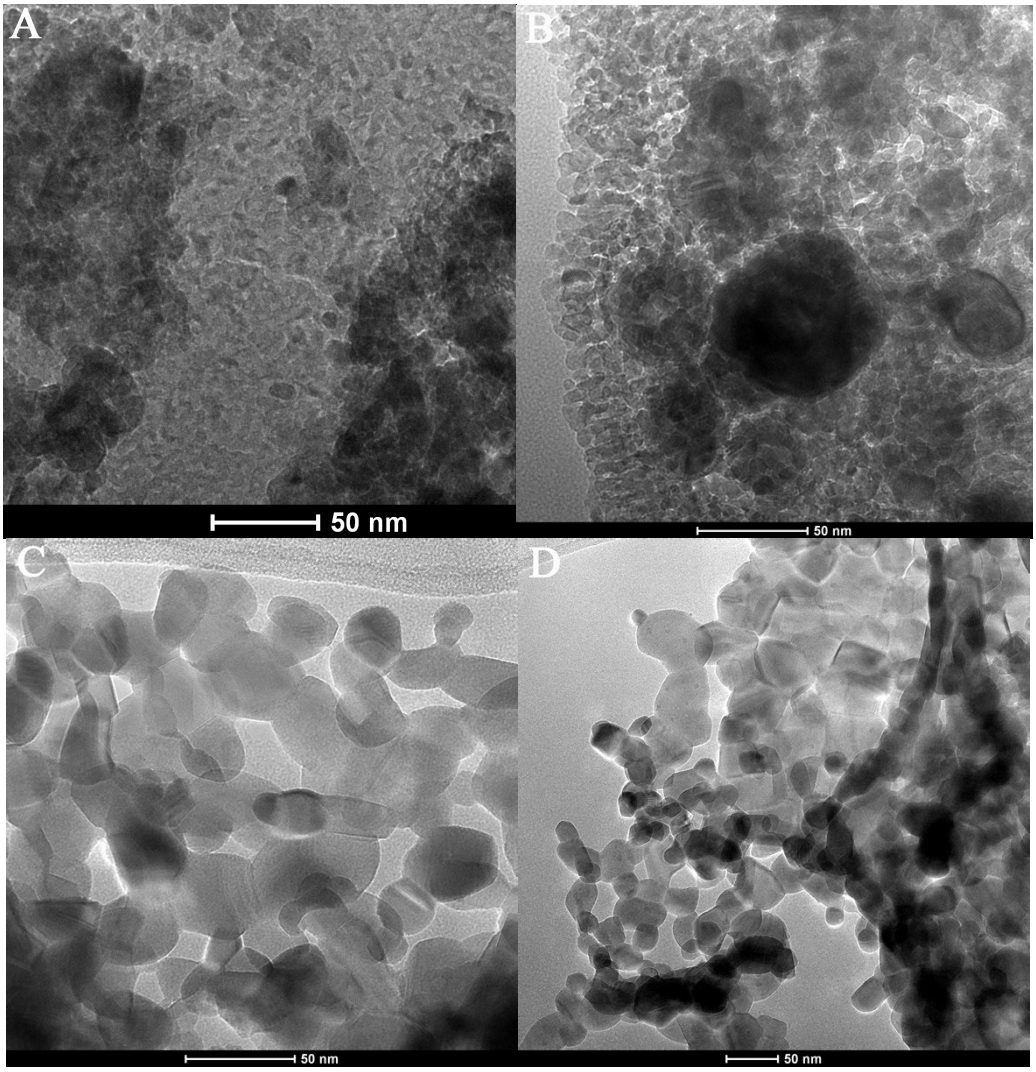

Figure S9. TEM images of the pre-reduced catalysts (A: re-45CZs and C: re-45CZs750) and used catalysts after esters hydrogenation (B: af-45CZs and D: af-45CZs750).

References

1. J. Evans, M. Wainwright, A. Bridgewater and D. Young, *Appl. Catal.,* 1983, **7,** 75-83.
2. S. Sato, R. Takahashi, T. Sodesawa, K. I. Yuma and Y. Obata, *J. Catal.*, 2000, **196,** 195-199.
3. C. Van Der Grift, A. Wielers, B. Jogh, J. Van Beunum, M. De Boer, M. Versluijs-Helder and J. Geus, *J. Catal.*, 1991, **131,** 178-189.
4. H. Boer, W. Boersma and N. Wagstaff, *Rev. Sci. Instrum.*, 1982, **53,** 349-361.
5. I. Melian-Cabrera, M. L. Granados and J. Fierro, *J. Catal.*, 2002, **210,** 285-294.
6. S. Xia, Z. Yuan, L. Wang, P. Chen and Z. Hou, *Appl. Catal., A*, 2011, **403**, 173-182.
7. X. Dong, H. B. Zhang, G. D. Lin, Y. Z. Yuan and K. R. Tsai, *Catal. Lett.*, 2003, **85,** 237-246.
8. J. Ahlers, J. Grasser, B. Loveless and D. Muggli, *Catal. Lett.*, 2007, **114,** 185-191.
9. H. Wilmer, T. Genger and O. Hinrichsen, *J. Catal.*, 2003, **215,** 188-198.

10. F. Arena, G. Italiano, K. Barbera, S. Bordiga, G. Bonura, L. Spadaro and F. Frusteri, *Appl. Catal., A*, 2008, **350,** 16-23.